Lagrangian diffusivity estimates from a gyre-scale numerical experiment on float tracking

Lagrangian diffusivity
Floats
Quasi-geostrophy
Numerical simulation
Eddies

Diffusivité lagrangienne
Flotteurs
Quasi-géostrophie
Simulation numérique
Tourbillons

Jacques VERRON, Kim Dan NGUYEN
Institut de Mécanique de Grenoble, BP 68, 38402 Saint-Martin d'Hères-Cedex, France.

Received 19/1/88, in revised form 6/9/88, accepted 24/10/88.

ABSTRACT

This paper reports the preliminary results of numerical experiments in which float tracking over the greatest part of an ocean basin was simulated during the equivalent of 300 days. The ocean model is a two-layer quasigeostrophic model and is fully eddy-resolving. The dynamical situation reproduced is typical of the unstable situation of mid-latitude ocean circulation, where an intense jet develops strong barotropic and baroclinic instabilities. Eddy activity itself drives recirculation patterns besides the surface jet. These mesoscale eddies are also responsible for downward propagation of energy, thereby inducing currents in the lower layer which contribute significantly to the total mass transport.

Numerical particle tracking is developed, together with algorithms adapted for the proper management of Lagrangian statistics. Recovery of the mean currents (and the eddy fields) at the basin scale is attempted by partitioning the Eulerian domain. The aim is to apply the Taylor concepts of dispersion after removing the Eulerian inhomogeneous component. The same idea is used in an attempt to map the diffusivity fields throughout the model ocean. Because intense wave activity competes with turbulence in a large part of the basin, attention is given to long-term effective diffusivities, which average the effects of wave stirring. The resulting diffusivities are matched against with the theoretical analysis of single-particle dispersion by Babiano *et al.* (1987).

Oceanologica Acta, 1989, **11**, 2, 167-176.

RÉSUMÉ

Estimation de la diffusivité lagrangienne à partir d'une expérience numérique de suivi de flotteurs

Cet article présente des résultats préliminaires d'une expérience numérique dans laquelle le suivi de « flotteurs » est simulé à l'échelle d'un bassin océanique pendant l'équivalent de 300 jours. Le modèle d'océan est quasi-géostrophique et résoud explicitement les tourbillons de moyenne échelle. On s'intéresse à une situation dynamique typique des circulations générales aux latitudes moyennes dans lesquelles se développent un jet intense et de fortes instabilités barotropes et baroclines. L'activité tourbillonnaire est en elle-même responsable d'une partie importante de la circulation moyenne de surface. De plus, les tourbillons de moyenne échelle assurent une propagation verticale de l'énergie en dessous du jet, et induisent des courants profonds qui contribuent de manière significative au transport total.

Le suivi numérique de flotteurs est réalisé dans le modèle afin d'en extraire des statistiques lagrangiennes pertinentes. La circulation générale moyenne et les champs de variabilité sont reconstitués à l'échelle du bassin après partition du domaine eulérien. L'idée est d'appliquer les concepts de Taylor sur la dispersion après avoir déduit la composante inhomogène du courant eulérien. De même, nous tentons de cartographier les champs de diffusivité à l'échelle du bassin. En raison de la compétition entre la dynamique turbulente et les ondes, l'intérêt est surtout porté sur la diffusivité à long terme qui moyenne l'effet de ces dernières. Les résultats sont confrontés avec l'analyse théorique de la dispersion des particules de Babiano *et al.* (1987).

Oceanologica Acta, 1989, **11**, 2, 167-176.

INTRODUCTION

Experiments with ocean floats, including surface drifters and SOFAR floats, have demonstrated the usefulness of this technique for documenting the oceanic general circulation and its mesoscale variability (Freeland *et al.*, 1975; Rossby *et al.*, 1975; Schmitz *et al.*, 1981; Richardson, 1981; 1983; Colin de Verdière, 1983; Riser and Rossby, 1983; Krauss and Böning, 1987). This is particularly true in the case of subsurface floats, which drift at a quasi-constant depth below the main thermocline, and constitute an important source of information on the field of eddy activity in the deep layers, which are not easily accessible by other means. They are an indispensable complement to other techniques like direct Eulerian or satellite measurement. Statistical analysis from float data may also provide information on particle dispersion and Lagrangian diffusivity, which deserve examination in relation to the variability field. These aspects are critical for achieving a better understanding of large-scale oceanic mixing and for developing a better parameterization of eddies in models, as well as for many chemical and biological studies.

However, this type of approach is inhibited in its ability to illuminate the general circulation because of the highly inhomogeneous and nonstationary nature of oceanic variability. Because the Eulerian currents are strongly varying at small (space and time) scales, the strategy of float deployement has to be optimized to extract the required information from the signal with a relevant statistical accuracy. As a result of these difficulties, and the growing availability of Lagrangian data, numerical simulation of particle motions in the ocean has been increasingly undertaken for purposes of interpretation and comparison. This has been rendered possible because of the recent development of eddy-resolving models of the ocean circulation. These models are beginning to provide an image of the ocean which has, in many respects, the gross features of the real coean, in particular the geography of the energy-containing variability. Although specific Lagrangian models exist, they are not currently widespread, and most eddy-resolving models use an Eulerian fixed grid. Consequently, Lagrangian data have to be obtained from further integration and interpolation techniques.

The present work falls into this category: we numerically integrate the Lagrangian trajectories from an Eulerian ocean circulation model and then use these integrations for recovering flow informations and extracting float dispersion statistics. The general objective is to study the geography of float dispersion and particle diffusivity in relation to the general basin-scale circulation and its mesoscale variability. In the second section we briefly describe the numerical experiment and the float tracking. In the third section we present diffusivity estimates and related quantities, firstly from a global point of view and secondly on the scale of the mean currents.

DESCRIPTION OF THE NUMERICAL EXPERIMENT

The model

The ocean model has two-layers and is quasigeostrophic and driven by a constant, double-gyre, wind-stress curl at the surface. The basic equations are written in terms of the streamfunction and vorticity for each layer. Details of the model formulation and of the geometry and parameters are provided elsewhere. Basically, the model is the one presented by Holland (1978), which has been extensively used. Because of its resolution and small dissipation it has the ability to exhibit strong instabilities and to give a picture of the ocean which is fully turbulent. The numerical parameters of the present experiment are given in Table 1. This set of parameters was shown to give a pattern of general oceanic circulation which broadly reproduces the aspects of the mean flow and the eddy fields in the North Atlantic (Schmitz and Holland, 1982). In particular, it can reproduce the structure of the deep eddy kinetic energy quite well, and a number of other eddy statistics also have realistic signatures.

Table 1
Model parameters for the float tracking numerical experiment.
Paramètres du modèle pour l'expérience numérique de suivi des flotteurs.

Wind forcing	Double-gyre pattern	$\tau_0 = 10^{-4}$ m^2/s^2
Domain geometry	Extension	4,000 km × 4,000 km
	Vertical structure	$H_1 = 1{,}000$ m
		$H_2 = 4{,}000$ m
Dissipation	Lateral friction (Biharmonic)	$A_4 = 8 \times 10^9$ m^4/s
	Bottom friction	$\varepsilon = 10^{-7}$ s^{-1}
Other physical parameters	Earth rotation	$f_0 = 9.3 \times 10^{-5}$ s^{-1}
		$\beta = 2 \times 10^{-11}$ (ms)$^{-1}$
	Reduced gravity	$g' = 0.02$ m/s^2
Discretization	Finite-difference method	$\Delta x = \Delta y = 23$ km
		$\Delta t = 4$ h

The float tracking experiment was started from the dynamical situation of a "statistically steady state", in which eddies and mean flow are in mutual balance. The strategy of float deployment involved regularly seeding the floats or Lagrangian particles over most of the basin extent and both layers. To our knowledge, there is still no rationalization to sustain definite release strategies in such inhomogeneous flows. Regular seeding seemed a pragmatic choice which permits further subsampling. The initial placement of the particles is shown in Figure 1: 506 floats per layer were deployed with a regular spacing of $5\Delta x$ (and $5\Delta y$), *i. e.* 115 km. Throughout the 300 days of integration, this gave a typical average of about 150 float-days of observations for each subdomain 115×115 km^2 and a total of 151800 float-days per layer. The density of observations was fairly regular except in the restricted surface jet area from where the initially seeded floats are rapidly ejected. The largest departures from the average are observed there and can locally drop to 50 float-days.

Interest is focused on the ("absolute") dispersion of individual particles, which is representative of the evolution of mean property distributions (Davis, 1983). The number of releases was limited mainly by computing constraints. However, first guesses of the required number of floats to access the mean flow may be estimated from elementary statistical considerations on the turbulent field, assuming homogeneity and stationarity. The number of float-days Nd may be expressed as:

$$\mathrm{N}d \approx \frac{2\mathrm{T}\langle u'^2 \rangle}{\langle (\langle u \rangle - \bar{u})^2 \rangle} \qquad (1)$$

where $\langle u \rangle - \bar{u}$ corresponds to the difference between the estimate of the mean flow $\langle u \rangle$, given along with the actual finite integration time and the limited number of floats, and the true mean value $\bar{u}$. T is the integral time scale, and $\langle u'^2 \rangle$ the eddy energy. The overbar denotes a time average and the brackets $\langle\ \rangle$ an ensemble average. This also assumes that the trajectories of all the particles within the subdomain under consideration are independent of each other, namely, that the eddy scales are greater than the separation of these particles. A crude estimation based on an integral time scale of 10 days and a level of eddy energy of 100 cm^2/s^2 (typical of a sub-tropical gyre) will give an error of 10% on the mean flow deduced from the complete float dataset. In the Gulf Stream area, the scale of inhomogeneity is of the order of magnitude of the sub-domain size (115 km). Moreover, the eddy energy may amount to several thousand cm^2/s^2. Therefore the precision on the mean flow will be much less accurate, and the number of float-days insufficient to properly access the mean flow. Based on the previous criterion, a reliable mean flow estimate in the Gulf Stream would require enormous quantities of data.

Following the float trajectories

The trajectory of each float is determined by the kinematic requirement that each float moves as the local fluid velocity, that is:

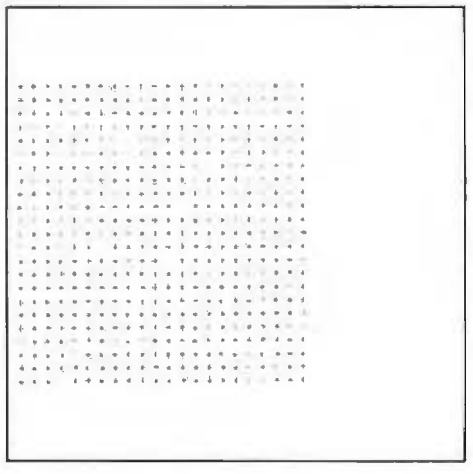

Figure 1
Sketch of the initial position of the 506 floats over the entire domain.
Répartition initiale des 506 flotteurs sur l'ensemble du bassin.

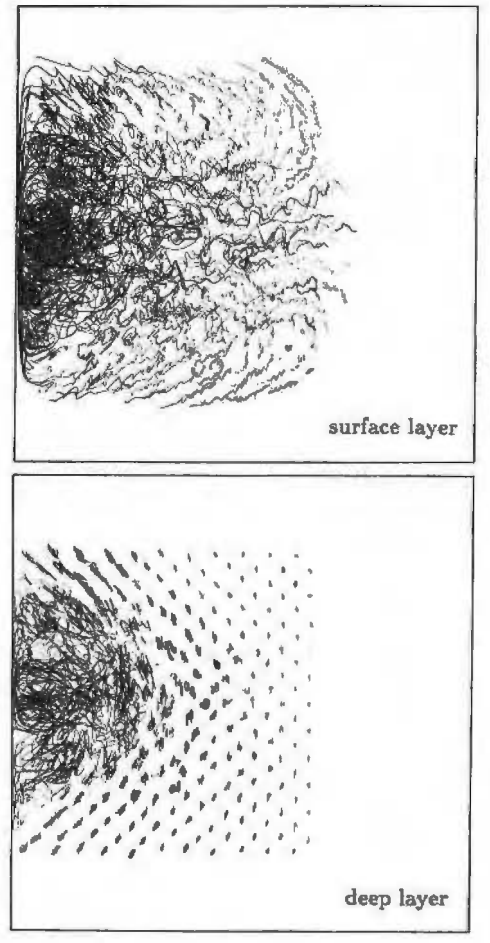

Figure 2
Spaghetti diagrams of float trajectories during the 300-day experiment.
Diagrammes spaghetti des trajectoires calculées pour les 300 jours de l'expérience.

$$\frac{dx_i}{dt} = u_i(x_i, t). \qquad (2)$$

Because the model has a fixed Eulerian grid, an interpolation procedure also has to be implemented for evaluating the velocity u_i (from the streamfunction field) at the position x_i which, in general, does not fit with in the grid. This is a second —in addition to the integration of (2)— source of computional inaccuracy. Figure 2 shows a "spaghetti diagram" of the computed trajectories during the time of the experiment.

Equation (2) is solved by a predictor-corrector, Newton-Raphson technique. The time-stepping for the integration is the model time-stepping, i.e., $\Delta t = 4$ h. Different methods have been tested for the interpolation scheme, including linear approximation, spline functions and weighted cubic functions. On test cases designed to best describe the float trajectories in the jet region, the last method appears to be the most accurate (De Floriani et Dettori, 1980). The numerical aspects of tracking Lagrangian particles into an Eulerian grid-point model have been discussed by Haidvogel (1982; 1986 unpublished manuscripts) and Babiano *et al.* (1987), in particular. They showed that the inaccurate conservation of potential vorticity along trajectories may not significantly affect the basic dispersion stastistics. However in their experiments,

Babiano *et al.* (1987) consider the estimates of single-particle dispersion might be biased due to numerical diffusion for time-scales larger than the integral time-scale.

ESTIMATES OF DIFFUSIVITY

Background

The basic ideas concerning particle dispersion come from the early works by Taylor (1921) and Kampé de Feriet (1939). The former was the first to establish the relationship between the trajectories of fluid parcels and the effective eddy diffusivity of the motion of the fluid.

Consider a set of particles, each particle having a Lagrangian horizontal velocity component defined as $u_i(t)$ ($i=1$ for zonal velocity, $i=2$ for meridional velocity). Let us assume that the turbulent flow field is homogeneous and stationary. It is useful to construct the Lagrangian correlation function R_{ij}:

$$R_{ij}=\langle u_i(t).u_j(t+\tau)\rangle. \tag{3}$$

This function measures the relation of the motion of the particle at time $t+\tau$ to the motion of the particle at time t. In other terms, it is a kind of measurement of the "memory" of the particle from its previous history. Moreover, stationarity implies that R_{ij} is only a function of τ. For short time ranges, this correlation is strong, but for large τ it has to be approaching zero while the particles are becoming decorrelated from the original position characteristics.

Taylor showed that a relation can be established between the diffusivity of the fluid parcels and the Lagrangian correlation:

$$k_{ij}=\frac{1}{2}.\frac{d}{dt}\langle x_i.x_j\rangle=\int_0^T R_{ij}(\tau).d\tau \tag{4}$$

where k_{ij} is the diffusivity $\langle x_i.x_j\rangle$, the dispersion of the particles, and T the duration of the experiment. As far as it is actually verified, this relationship could provide us with two possible ways of computing diffusivities form the statistics of an ensemble of float trajectories.

If the integration time is long enough, we can expect the integral value to reach a constant:

$$\int_0^\infty R_{ij}.d\tau=T_{ij}.\langle u_i.u_j\rangle=\lim_{T\to\infty}k_{ij} \tag{5}$$

where T_{ij} is the Lagrangian integral time scale. Under this condition, the diffusivity k_{ij} is also expected to reach a constant value along the direction given by the subscripts. Moreover, the diagonal terms appear to be directly related to the kinetic energy field.

Relation (4) is valid even when a mean flow is present. If $\langle x_i'.x_j'\rangle$, which represents the dispersion of the particles from their mean position, replaces $\langle x_i.x_j\rangle$, and the mean velocity is removed from the particle velocity, it also applies for the fluctuations. But in that case, the motion of the centre of gravity over all the floats must respect a linear law:

$$\frac{d\langle x_i\rangle}{dt}=\bar{u}_i=\langle u_i\rangle. \tag{6}$$

Use of this formula may be valid as long as the number of independent floats is large enough.

In the oceanic case, where homogeneity and stationarity assumptions are definitely not appropriate, it is still tempting to borrow some of the concepts of this fairly simple analysis. A crude way to manage inhomogeneity is to consider a version of (4) in which the time-mean component has been removed. But, for an inhomogeneous field of diffusivity, a difference exists between Eulerian and Lagrangian mean flow. Even in the absence of any Eulerian component the particles tend to move preferentially towards regions of larger diffusivities. An additional mean velocity is thus conjugated with the Eulerian velocity which may be derived as (Rossby *et al.*, 1983; Davis, 1987):

$$\langle u_i\rangle^*=\frac{\overline{\partial k_{ij}}}{\partial x_j}. \tag{7}$$

Therefore, any removal of the mean field by using the centre of mass will involve such mixed spatial interplay. The assumption of stationarity might be less constraining, because the most energetic eddies have time scales short enough compared to the duration of a typical experiment.

In Figure 3 we have drawn the motion of the centre of gravity issuing from our experiment. The two components of the dispersion $\langle x_1\rangle$ and $\langle x_2\rangle$ are sketched as a function of time for both layers. Although incomplete, the agreement towards linearity and (6) is quite correct. Given the symmetry of the problem, we could expect a zero value for the meridional component of the mean velocity. Notice that, because of non-linearity

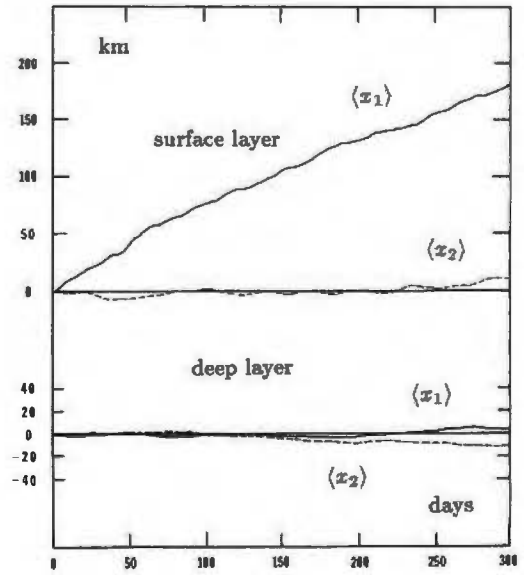

Figure 3
Components of the motion of the centre of mass of all floats.
Composantes du mouvement du centre de gravité de l'ensemble des flotteurs.

Table 2
Results of the global statistics analysis.
Résultats de l'analyse statistique globale.

		Surface Layer	Deep Layer
$\langle u_1 \rangle$	cm/s	0.60	0.01
$\langle u_2 \rangle$	cm/s	0.01	−0.04
$\langle u_1'^2 \rangle$	cm^2/s^2	71.9	18.6
$\langle u_2'^2 \rangle$	cm^2/s^2	71.8	24.7
k_{11}	10^7 cm^2/s	3.5*	1.0*
		3.1**	0.6**
k_{22}	10^7 cm^2/s	2.6*	0.9*
		2.1**	0.5**
T_{11}	day	5.6	6.2
T_{22}	day	4.2	4.2

* estimates from the right side of Eq. (4).
** estimates from the left side of Eq. (4).

and numerical noise, symmetry does not stand for instantaneous field, but only for the mean. The small nonzero values found (*see* also Table 2) show that the eddy-driven mean transport between the two gyres is still unbalanced when integrated over one year. This is clearly a residual effect of the nonstationarity of the statistics of the flow during the time scale under consideration. The zonal component of the mean velocity is due to the coverage of the initial float seeding: the jet region is favoured at the expense of the large Sverdrup return flow

Estimating the mean flow

We have mapped the estimated Eulerian mean velocities from the float data. We divided the basin into subdomains, each of which is centered on the initial position of float placement (Fig. 1) and has dimensions of $5\,\Delta x \times 5\,\Delta y$. Then on each subdomain, an Eulerian velocity can be deduced from the ensemble-average of all float-day velocities over the subdomain area. If the eddy variability were homogeneous and stationary, the time-averaged flow would be equal to the instantaneous average over distributed flow velocities. But in a real flow, where eddy energy varies in space, some error arises, as we mentioned before, from the fact that the centre of mass of the float ensemble moves up the gradient of turbulent energy. The chosen dimension ($5\,\Delta x \times 5\,\Delta y$) results from a compromise between the tendency to have small subdomains, which leads to a better representation of the velocity gradients, and the constraint on having sufficient information from floats and statistical convergence. In the recirculation region besides the jet stream, typical statistics give a plateau for the velocity estimate in the range of ($5\,\Delta x \times 5\,\Delta y$) to ($8\,\Delta x \times 8\,\Delta y$) subdomain size. The statistics are computed with a time interval of one day.

The resulting streamfunction was inferred by using a direct integration scheme from the estimated velocity over each subdomain (De Floriani and Dettori, 1980). Figure 4 shows maps of the streamfunction fields. The

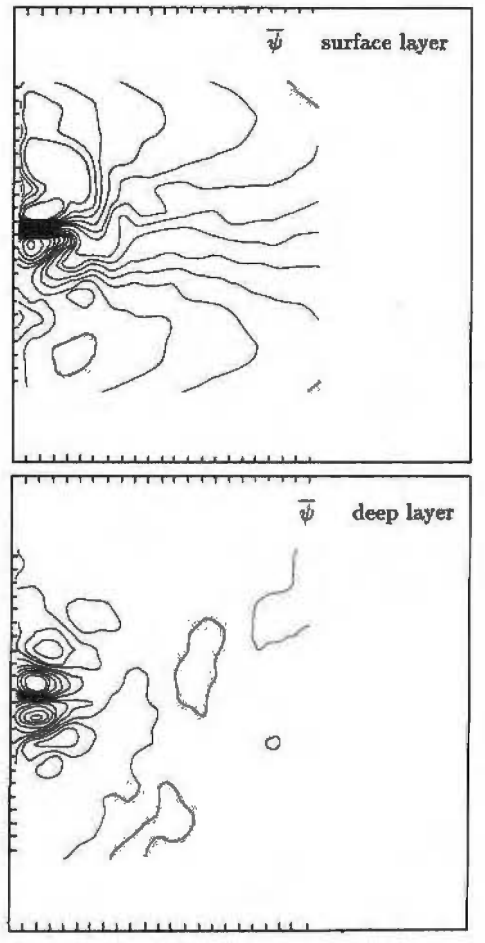

Figure 4
Mean streamfunction fields estimated from float data. Surface layer CI = 5,000 m^2/s, deep layer CI = 2,500 m^2/s.
Champs moyens des fonctions de courant estimés à partir des vitesses des flotteurs. En surface CI = 5 000 m^2/s; au fond CI = 2,500 m^2/s.

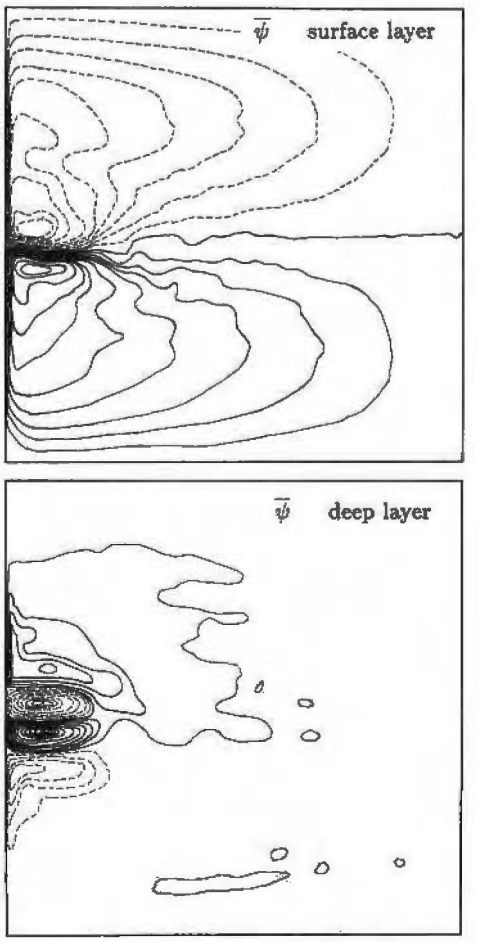

Figure 5
Mean streamfunction fields issuing from the model integration over five years of statistical steady state. Same CI as Figure 4.
Champs moyens des fonctions de courant obtenus par intégration du modèle sur cinq années en régime statistiquement stationnaire. CI comme sur le figure 4.

maps can be compared with the "real mean field", *i. e.* resulting independently from the model integration (Fig. 5). In the following we referred to this model field as the "real" field. Comparison between Figures 4 and 5 shows that better agreement is observed for the far field in the upper layer. In the deep layer, the flow is very much confined to the western boundary but the agreement is correct for the jet characteristics. The maximum transport in the upper-layer northern gyre is evaluated at about 40 Sv (1 Sv = 10^6 m^3/s), when it is 45 Sv in the southern gyre. This underestimates the "real" value by about 10%. In the deep layer the maximum transport is around 15 Sv in each inner gyre, which is close to the "real" value given the accuracy of the evaluation. One can observe a significant discrepancy from the symmetrical situation, especially in the surface flow. This can be related to the incomplete stationarity of the statistical sample but clearly also from inaccuracy in recovering the mean flow. Even discarding the estimation uncertainty coming from the floats, one year is notoriously insufficient for reaching complete stability in accessing the mean flow (Holland and Rhines, 1980). The bias in the mean flow estimate due to the spatially varying eddy intensity is difficult to estimate. Following (7) it would induce a spurious component of velocity $\langle u_i \rangle^*$ which may reach up to some 5 cm/s in the western area of the jet.

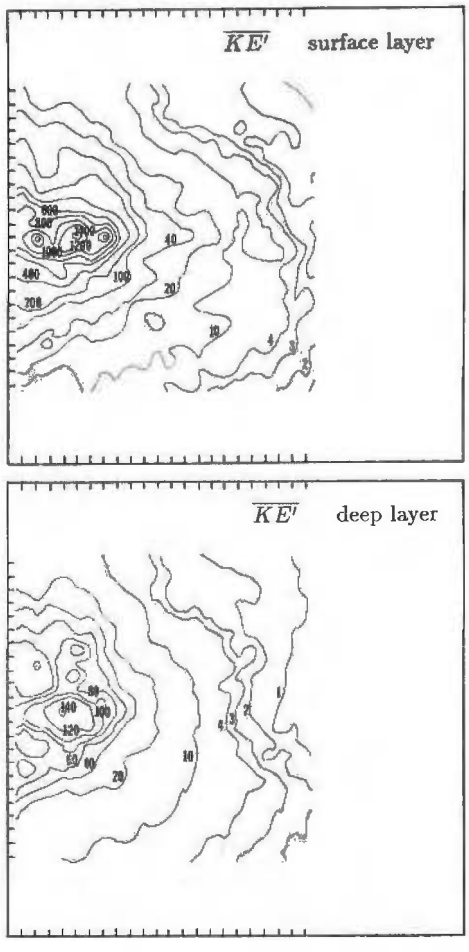

Figure 6

Mean eddy kinetic energy fields estimated from float data. CI as indicated. Units are cm^2/s^2.

Champs moyens de l'énergie cinétique tourbillonnaire (en cm^2/s^2) estimés à partir des vitesses des flotteurs. CI comme indiqué.

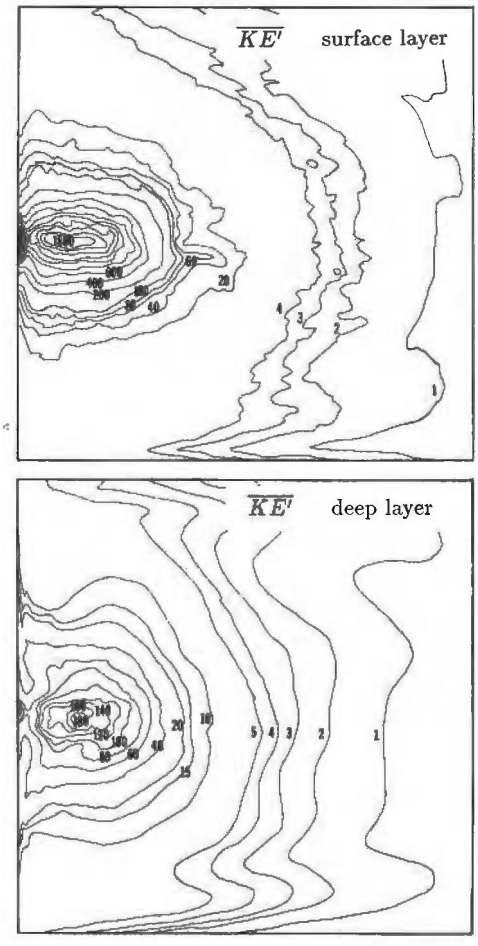

Figure 7

Mean eddy kinetic energy fields issuing from the model integration over five years of statistical steady state. CI as indicated. Units are cm^2/s^2.

Champs moyens de l'énergie cinétique tourbillonnaire (en cm^2/s^2) obtenus par intégration du modèle sur cinq années en régime statistiquement stationnaire. CI comme indiqué.

Elsewhere the effect is likely to be weak. The integrated effect of the streamfunction may dissimulate inaccuracy for determining the velocity field for the general circulation. On Figure 4, the circulation has some "realistic" flavor but the velocity estimate may be locally imprecise, especially in the Gulf Stream.

The kinetic energy field (Fig. 6 and 7) is recovered with better accuracy. This is consistent with the shortest time-scales associated with energy-containing eddies. The resolution of the float-analysis partitioning is still insufficient to reproduce all the details and especially the most intense gradients. This leads to an underestimation of the very concentrated maximum values for the eddy energy. But the low levels are remarkably well reproduced, which confirms *a posteriori* the accuracy of the mean flow velocity removal in these regions.

Basin-scale statistics

The float mean velocity previously estimated has been subtracted from the data and the residual fluctuation series were used to compute a global covariance tensor. The uncertainty on the computed mean flow has limited consequence on the variability estimation because the eddy energy clearly exceeds the mean over most of the basin, especially in the regions where the mean is

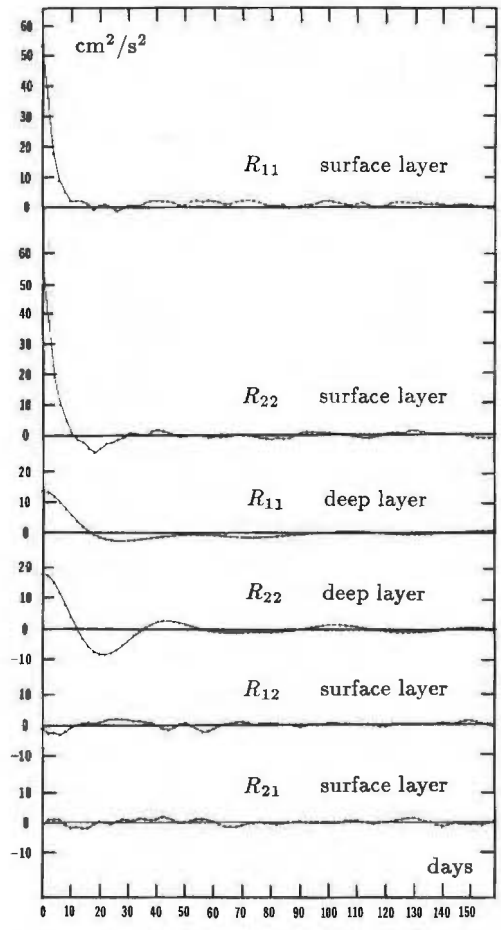

Figure 8

Lagrangian correlation R_{11}, R_{22}, R_{12}, and R_{21} as a function of time in both layers for the global set of float days.

Corrélation lagrangienne R_{11}, R_{22}, R_{12} et R_{21} en fonction du temps dans les deux couches pour toute la durée de l'expérience.

doubtful. Figure 8 shows the autocorrelations R_{11} and R_{22} as well as the cross-correlations R_{12} and R_{21}. R_{11} and R_{22} look similar in both layers. Zero-crossing is about 17 days for R_{11} in both layers compared to about ten days and 12 days for R_{22}, at the surface and in the deep flow, respectively. These time-scales have to be examined by reference to the Lagrangian integral time scales of Table 2, which are appreciably shorter although with similar anisotropy. The anisotropy is also visible through the presence of negative correlations which are much more pronounced for R_{22}. Wave oscillations are clearer in the deep layer because of the relatively larger importance of wave energy. The parabolic departure from the origin is clearly observed in the deep layer, and probably also present in the surface layer although somewhat masked by the sharp decrease in our figure. This is in accordance with the autocorrelation derivation within the Taylor framework assuming only the acceleration are finite (Freeland *et al.*, 1975).

Following (4) for small times after launch the dispersion varies as:

$$\langle x_i'^2 \rangle \sim t^2 . \langle u_i'^2 \rangle \qquad (8)$$

while at large times (4) and (5) give:

$$\langle x_i'^2 \rangle \sim 2t . T_{ii} . \langle u_i'^2 \rangle . \qquad (9)$$

These relations are classically used for giving a model of the dispersion.

Fluctuation series are also used for computing global estimates for the Lagrangian diffusivity k_{ij}. This has been done in two ways according to the two sides of the Taylor equation (4). Results for k_{11} and k_{22} are presented in Figure 9 for each layer. A certain discrepancy exists between the two estimates, which is not really surprising when we recall that the ocean model does not follow the basic Taylor assumptions. In particular, oceanic turbulence in the Gulf Stream area is strongly inhomogeneous and anisotropic. The computed discrepancy has the property of being fairly constant and larger for the k_{22} estimates. The mean velocity induced by the diffusivity gradient certainly accounts for a part of the difference because the velocity gradients in the jet stream have stronger anisotropy in the meridional direction. The smoothing effect of the spatial averaging is also disadvantageous. Beyond a typical eddy time scale ($\approx$20 days), the evolution of k_{ii} in time is reaching a plateau. In the second layer, the relatively stronger importance of waves can be clearly seen. But in a general way the k_{ii} values are found to converge fairly well towards a constant value. This a posteriori validates the process of removing the Eulerian value.

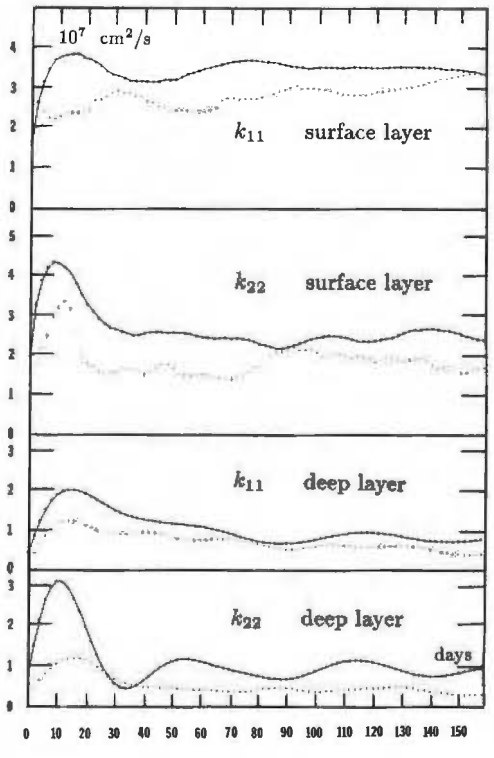

Figure 9

Global estimates of the diffusivity k_{11} and k_{22} as a function of time in both layers for the global set of float days. Solid lines are for computations according to the right side of equation (3)*, dashed lines for the left side.*

Estimations globales de la diffusivité k_{11} et k_{22} en fonction du temps dans les deux couches pour toute la durée de l'expérience. Les résultats sont en pointillés pour le premier membre de l'équation (4) et en trait continu pour le second membre.

Large-scale diffusivity estimates

The same computing procedure as above has been applied in dividing the domain into 25 (5×5) regions of investigation. The size of each region is then $25\,\Delta x \times 25\,\Delta y$, *i.e.* 575×575 km^2. Moreover, in order to increase amount of relevant information within each sub-domain, we have divided the original trajectories by 20-day intervals, *i.e.*, a time-scale larger than the decorrelation time. Statistical stability in estimating local diffusivity necessitated such increase in sub-domain size and trajectory subsampling. Within each region, we make the simplifying assumptions of statistical homogeneity and stationarity, and consider the different float tracks as being equivalent to a large number of tracks originating from the same location and differing only in the time of launch. As previously, the mean velocity as estimated from the local floats is subtracted.

As expected, the estimates for the diffusivity coefficient are strongly time-dependent as well as space-dependent (including vertical). We can roughly identify two extreme types of behaviour:

– In the jet area, the k_{ii} evolution in time has a general trend towards constant values. A spurious effect may be present especially in the most western area when particles may be swept along by the boundary current.

– In the "open ocean", the k_{ii} evolution is wave-like for the larger times, and the definition of k_{ii} is definitely subject to the choice of a time scale. The duration of our experiment is long enough compared to a typical wave period (of the order of 40 days) to allow time-averaging. The average gives an estimate for long-term diffusivity, which is expected to be the effective diffusivity. Instantaneous values are generally much larger than this mean and may be strongly negative. But they give a picture of the local stirring rather than a measure of the particle dispersion.

The resulting diffusivity fields have been drawn in Figure 10 on the preceding basis of time-average long-term diffusivity. These fields must be examined keeping in mind the fact that resolution is somewhat crude. The similarities with the eddy kinetic-energy patterns are apparent, with two notable exceptions: the location of the maximum k_{ii} values is shifted westward by reference to the energy field, and two more intense patches of k_{22} appear besides the surface jet. But these areas are precisely the very regions where our computational assumptions of homogeneity and stationarity are the less relevant. Therefore these particular features have to be considered cautiously. Otherwise we notice that the long-term diffusivity is not significantly distinguishable from zero (given the accuracy of the statistics) in the bulk of the deep flow.

Some measurements (Rossby *et al.*, 1983) have suggested a linear relationship between k_{ii} and $\overline{u_i'^2}$ which would imply, within the Taylor theory, a constant integral time scale over the basin. Figure 11 shows such presentation of k_{ii} *versus* $\overline{u_i'^2}$ in the case of our numerical results. Experimental data mentioned by Rossby *et al.* (1983) have also been indicated. In both layers we may consider that the data have a tendency to be distributed over a power law. Such power law $k_{ii} \sim (\overline{u_i'^2})^{\alpha}$ will correspond to a Lagrangian time scale:

$$T_{ii} \sim (\overline{u_i'^2})^{\alpha - 1} \qquad (10)$$

which gives a constant time scale T_{ii} for $\alpha = 1$. In the surface layer, the slope α of the log-log diagram may be viewed as close to the value of 1, although a weaker slope may be more relevant for a broad range of data in the zonal direction. More specific examination shows effectively no clear tendency for T_{22} to be dependent on $\overline{u_2'^2}$. On the other hand, T_{11} is found to be related to $\overline{u_1'^2}$, especially with a clear increase of the Lagrangian time scale for the low-energy levels. In that case an appropriate value, if any, for α will certainly be less

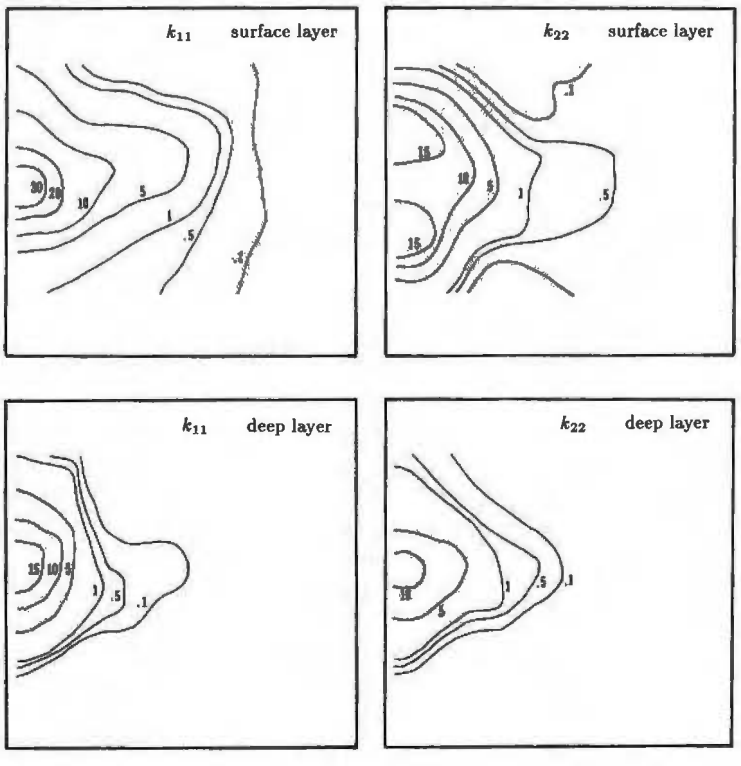

Figure 10

Schematic maps of the diffusivity fields k_{11} and k_{22} in both layers over the domain. CI as indicated. Units are 10^7 cm^2/s.

Cartographie des champs de diffusivité k_{11} et k_{22} (en 10^7 cm^2/s) dans les deux couches sur l'ensemble du bassin. CI comme sur les figures 4 à 7.

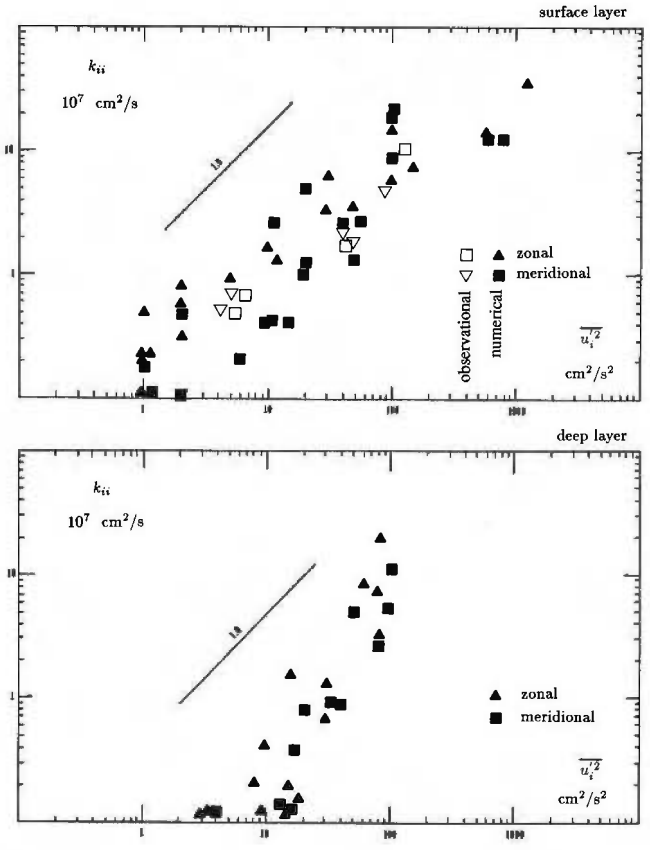

Figure 11

Relation between diffusivity and eddy kinetic energy in both layers.

Relation entre la diffusivité et l'énergie cinétique tourbillonnaire dans les deux couches.

than 1. In the deep flow, on the other hand, we observe an increase in the slope α (Fig. 11). It would correspond to a Lagrangian time scale increasing with $\overline{u_i'^2}$. For the widest part of the $(k_{ii}, \overline{u_i'^2})$ parameter range under consideration, the dynamics is more wave-like than turbulent, which makes a noticeable difference from the surface layer. The presence of Rossby waves is highlighted in both layers by the enhancement of the zonal dispersion to the detriment of the meridional dispersion. The effects of turbulence and Rossby waves are intricated all over the basin. Therefore, in a global ocean basin such as ours, where the geography of the variability is complex, we could not expect necessarily a uniform and simple dependency of the Taylor kind. Let us also recall that because the wave-like activity is stronger there, the uncertainty of our estimation is further increased. Last but not least, we must mention that the effect of bottom friction is essential in draining an important part of the eddy kinetic energy and may account for this peculiar behaviour of the deep layer.

Another rationalization was proposed by Babiano *et al.* (1987; 1988) who develop theoretical expression for single-particle dispersion and eddy diffusion. The Taylor classical concepts are extended to the whole self-similar range of the Lagrangian energy spectrum. At times much larger than the Lagrangian time scale the diffusivity is expressed as:

$$k = \sqrt{\frac{8\pi}{3}} E Z^{-1/2} \qquad (11)$$

where E is the eddy energy and Z a generalized enstrophy

$$\left(Z = \frac{1}{4} \left\langle \left(\frac{\partial v}{\partial x} - \frac{\partial u}{\partial y} \right)^2 + \left(\frac{\partial u}{\partial x} - \frac{\partial v}{\partial y} \right)^2 + \left(\frac{\partial v}{\partial x} + \frac{\partial u}{\partial y} \right)^2 \right\rangle \right).$$

The comparison between this theoretical expression and the present numerical results is shown on Figure 12. A rough agreement is observed in the range of larger k in the surface layer, more precisely in the subregions besides the surface jet where the eddy activity is strong and relatively isotropic. The theoretical prediction overestimates the diffusivity in the range of smaller values corresponding to more quiet regions. These are also the regions where wave dynamics strongly affect the local diffusivity and may spuriously influence our numerical estimation. In the deep layer the theoretical prediction is far from satisfying, again probably because of the frictional effect.

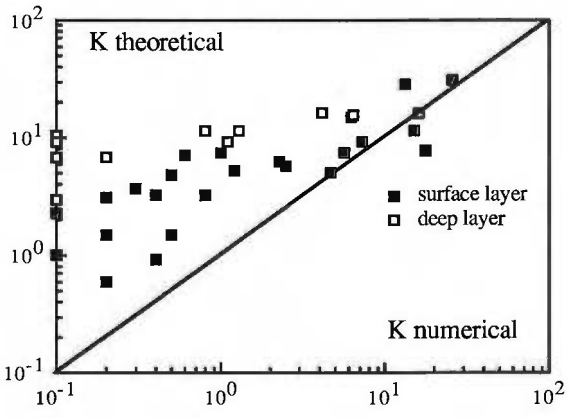

Figure 12

Comparison between present results on the diffusivity k and prediction by Babiano et al. (1987). *Units are* 10^7 *cm²/s.*

Comparaison entre les valeurs de diffusivité k (en 10^7 cm²/s) obtenues dans le présent travail et celles fournies par Babiano *et al.* (1987).

CONCLUSION

In this work we have attempted to simulate the ability of Lagrangian float tracking to recover the general features of oceanic circulation at basin scale, and more specifically to assess the Lagrangian absolute diffusivity field by using Taylor concepts on dispersion. The conditions in which numerical investigation has been undertaken are successful enough to permit an accurate recovery of the mean flow properties. Using the mean flow estimates, we have presented, in the second part, the results of a tentative mapping of basin-scale diffusivity. Strong geographical variation of diffusivity is observed in accordance with the variability of the dynamics over the basin. Several difficulties arose which in great measure originated in numerical limitations. According to observational standards, the number of float-days (151800×2) we have used is large. But *a posteriori* our results would have strongly benefited from denser deployment to allow finer partition of the Eulerian domain. This requirement would have been necessary to test more accurately some rationalization such as those suggested by certain measurements *in situ* or theoretical developments. In the surface layer,

our results show that the Lagrangian time-scale is not too far from being constant all over the basin. In a limited range of dynamical conditions corresponding to the recirculation regions of the jet stream, the theoretical prediction by Babiano *et al.* (1987) is close to the numerical estimates. However, at basin scale, the joint action of turbulence and waves may make it difficult to point out a simple relationship which remains valid for the whole gyre. Compared to the surface, deep float statistics reveal significant differences whose origin is obscure. The effect of stratification and the possible bias due to bottom friction call for clarification in a further simulation using a higher number of layers in the model.

Acknowledgements

We wish to acknowledge helpful conversations with Dale Haidvogel and useful referees' comments. Calculations were made with the numerical facilities of the *Centre de Calcul Vectoriel pour la Recherche* in Palaiseau. Completion of this work has been done when JV was visiting scientist at the National Center for Atmospheric Research under the United States-France exchange programme, which is sponsored by the National Science Foundation and the *Centre National de la Recherche Scientifique* (CNRS).

REFERENCES

Babiano A., C. Basdevant, P. Le Roy and R. Sadourny (1987). Single particle dispersion, Lagrangian energy spectrum in two-dimensional incompressible turbulence. *J. mar. Res.*, **45**, 107-131.

Babiano A., C. Basdevant, P. Le Roy and R. Sadourny (1988). Relative dispersion in two-dimensional incompressible turbulence (in preparation).

Colin de Verdière A. (1983). Lagrangian eddy statistics from surface drifters in the eastern North Atlantic. *J. mar. Res.*, **41**, 375-398.

Davis R. E. (1983). Oceanic property transport, Lagrangian particle statistics and their prediction. *J. mar. Res.*, **41**, 163-194.

Davis R. E. (1987). Modelling eddy transport of passive tracers. *J. mar. Res.*, **45**, 635-666.

De Floriani L. and G. Dettori (1980). Surface interpolation methods over rectangular and triangular grids. In: *Numerical methods for Engineering*, E. Arsi, R. Glowinsky, P. Lascaux and H. Vesseyre, editors, Dunod, Paris, pp. 12-31.

Freedland H. J., P. B. Rhines and H. T. Rossby (1975). Statistical observations of the trajectories of neutrally buoyant floats in the North Atlantic. *J. mar. Res.*, **33**, 383-403.

Holland W. R. (1978). The role of mesoscale eddies in the general circulation of the ocean. Numerical experiments using a wind-driven quasigeostrophic model. *J. phys. Oceanogr.*, **8**, 363-392.

Holland W. R. and P. B. Rhines (1980). An example of eddy-induced ocean circulation. *J. phys. Oceanogr.*, **10**, 1010-1031.

Kampé de Feriet J. (1939). Les fonctions aléatoires stationnaires et la théorie statistique de la turbulence homogène. *An. Soc. cient. Bruxelles*, **59**, 145-194.

Krauss W. and C. W. Böning (1987). Lagrangian properties of eddy fields in the northern North Atlantic as deduced from satellite-tracked buoys. *J. mar. Res.*, **45**, 259-291.

Richardson P. L. (1981). Gulf-Stream trajectories measured with free-drifting buoys. *J. phys. Oceanogr.*, **11**, 999-1010.

Richardson P. L. (1983). Eddy kinetic energy in the North Atlantic from surface drifters. *J. Geophys. Res.*, **88**, 2705-2709.

Riser S. C. and H. T. Rossby (1983). Quasi-Lagrangian structure and variability of the subtropical Western North Atlantic circulation. *J. mar. Res.*, **41**, 127-162.

Rossby H. T., A. D. Voorhis and D. C. Webb (1975). A quasi-lagrangian study of mid-ocean variability using long range SOFAR floats. *J. mar. Res.*, **33**, 355-382.

Rossby H. T., S. C. Riser and A. J. Mariano (1983). The western North Atlantic. A Lagrangian viewpoint. In: *Eddies in Marine Science*, A. R. Robinson, editor, Springer-Verlag.

Schmitz W. J. and W. R. Holland (1982). A preliminary comparison fo selected numerical eddy-resolving general circulation experiments with observations. *J. mar. Res.*, **40**, 75-117.

Schmitz W. J., J. F. Price, P. L. Richardson, W. B. Owens, D. C. Webb, R. E. Cheney and H. T. Rossby (1981). A preliminary exploration of the Gulf Stream system with SOFAR floats. *J. phys. Oceanogr.*, **11**, 1194-1204.

Taylor G. I. (1921). Diffusion by continuous movements. *Proc. Lond. Math. Soc.*, **20**, 196-212.